# Nonlinear dielectric spectroscopy in the smectic-$A$–smectic-$C^*_\alpha$ phase transition

Andika Fajar, Hidetoshi Murai, and Hiroshi Orihara
*Department of Applied Physics, Graduate School of Engineering, Nagoya University, Furo-cho, Nagoya 464-8603, Japan*
(Received 2 April 2001; published 28 March 2002)

We performed nonlinear dielectric spectroscopy to study the dynamic properties near the smectic-$A$–smectic-$C^*_\alpha$ phase transition point of an antiferroelectric liquid crystal 4-(1-methyl-heptyloxycarbonyl)phenyl 4-octylcarbonyloxybiphenyl-4-carboxylate (MHPOCBC). A Landau-type theory was developed in order to analyze the experimentally obtained frequency dispersions. From the experimental and theoretical results we successfully obtained the temperature dependence of the relaxation frequency of the soft mode in both the smectic-$A$ and smectic-$C^*_\alpha$ phases, which gave direct evidence that the transition is brought about by soft mode condensation. Significant features of this transition are also discussed.

DOI: 10.1103/PhysRevE.65.041704 PACS number(s): 61.30.−v, 64.70.Md, 64.60.Ht

## I. INTRODUCTION

Several intermediate phases, the so-called Sm-$C^*_\alpha$ and some ferrielectric phases, have been found in chiral smectic liquid crystals in addition to the antiferroelectric Sm-$C^*_A$ phase. Among them, the Sm-$C^*_\alpha$ phase has attracted much attention because of its unique physical properties. This phase usually appears between the well known paraelectric Sm-$A$ and ferroelectric Sm-$C^*$ phases, and in some compounds between Sm-$A$ and Sm-$C^*_A$ or ferrielectric phases. Early experiments revealed that the Sm-$C^*_\alpha$ phase is a tilted phase with small molecular tilt angle and its magnitude increases smoothly with decreasing temperature [1,2]. Recently, resonant x-ray scattering measurements indicated that the Sm-$C^*_\alpha$ phase has a short-pitch ferroelectriclike structure and the period is incommensurate with the smectic layer spacing [3,4]. Therefore, the Sm-$C^*_\alpha$ phase is considered to be formed by condensation of the soft mode located at a general point of the smectic Brillouin zone in the Sm-$A$ phase. In general, the observation of the soft mode is quite important in elucidating the mechanism of phase transitions. In the Sm-$A$–Sm-$C^*$ phase transition the soft mode has been observed by means of dielectric and photon correlation spectroscopies [5,6]. However, for the Sm-$A$–Sm-$C^*_\alpha$ phase transition it is difficult as will be explained later.

Here, let us briefly explain the collective orientational modes related to the present study. They are illustrated in Fig. 1. In the Sm-$A$ phase, the soft mode is a helically tilting mode with a short pitch corresponding to the structure of the Sm-$C^*_\alpha$ phase. Its condensation brings about the Sm-$A$–Sm-$C^*_\alpha$ phase transition. In addition to this, we have a homogeneously tilting mode, called the ferroelectric mode, which induces macroscopic polarization due to the electroclinic effect. Therefore, this mode can be directly excited by an electric field. The ferroelectric mode becomes the soft mode in the case of the Sm-$A$–Sm-$C^*$ phase transition (strictly speaking, the soft mode is not exactly located at the smectic Brillouin zone center, but close to the zone center to produce a long-period helix in the Sm-$C^*$ phase). These modes modify the dielectric tensor or the indicatrix, as shown at the bottom of the figure. In particular, the soft mode modifies the birefringence, but it should be noted that the birefringence change is proportional to the square of the amplitude of the soft mode (the tilt angle). In the Sm-$C^*_\alpha$ phase, on the other hand, the doubly degenerate soft mode in the Sm-$A$ phase changes into an amplitude mode and a phase mode. The amplitude mode modifies the tilt angle, while the phase mode (the Goldstone mode) modifies the azimuthal angle, i.e., the spatially homogeneous rotation of molecules around the layer normal. The amplitude mode becomes soft as the transition point is approached in the Sm-$C^*_\alpha$ phase, while the relaxation frequency of the phase mode is always zero. The ferroelectric mode still exists in the Sm-$C^*_\alpha$ phase, which produces macroscopic polarization as in the Sm-$A$ phase. Note that the dielectric tensor can be modified both by the amplitude mode and the ferroelectric mode, but not by the phase mode. In particular, the birefringence change is proportional to the amplitude of the amplitude mode (the change of the tilt angle). This is different from the change for the soft mode in the Sm-$A$ phase and easily understood as follows. From symmetry considerations the birefringence change $\Delta n_a$ may be proportional to the square of the amplitude of the soft mode (the tilt angle), $\xi$, in the Sm-$A$ phase, i.e., $\Delta n_a \propto \xi^2$. In the Sm-$C^*_\alpha$ phase the spontaneous tilt $\xi_s$ appears and therefore $\Delta n_a \propto (\xi_s+\Delta\xi)^2 \doteqdot \xi_s^2 + 2\xi_s\Delta\xi$ for small $\Delta\xi$, where $\Delta\xi$ is the amplitude of the amplitude mode.

Since the soft mode related to the Sm-$A$–Sm-$C^*_\alpha$ phase transition is located at a general point in the smectic Brillouin zone, it is difficult to observe it experimentally. In the Sm-$C^*_\alpha$ phase, however, the soft mode changes into an amplitude mode and a phase mode, located at the Brillouin zone center, and the change of the birefringence due to the amplitude mode is proportional to $\xi_s\Delta\xi$. Therefore, the amplitude mode can be observed. In fact, it has been observed by means of second-order electro-optical spectroscopy [7]. In the electro-optic response the nonlinear coupling between the soft mode and the ferroelectric mode plays an important role as will be shown in Sec. II. When we apply an electric field, first the ferroelectric mode is excited and then the soft mode through the nonlinear coupling. As a result, from symmetry considerations it is easily seen that the amplitude mode is excited as $\Delta\xi \propto E^2$, where $E$ is the applied field, resulting in the Kerr effect. Although the observation of the soft mode is difficult in the Sm-$A$ phase, it is not entirely impossible if we

 

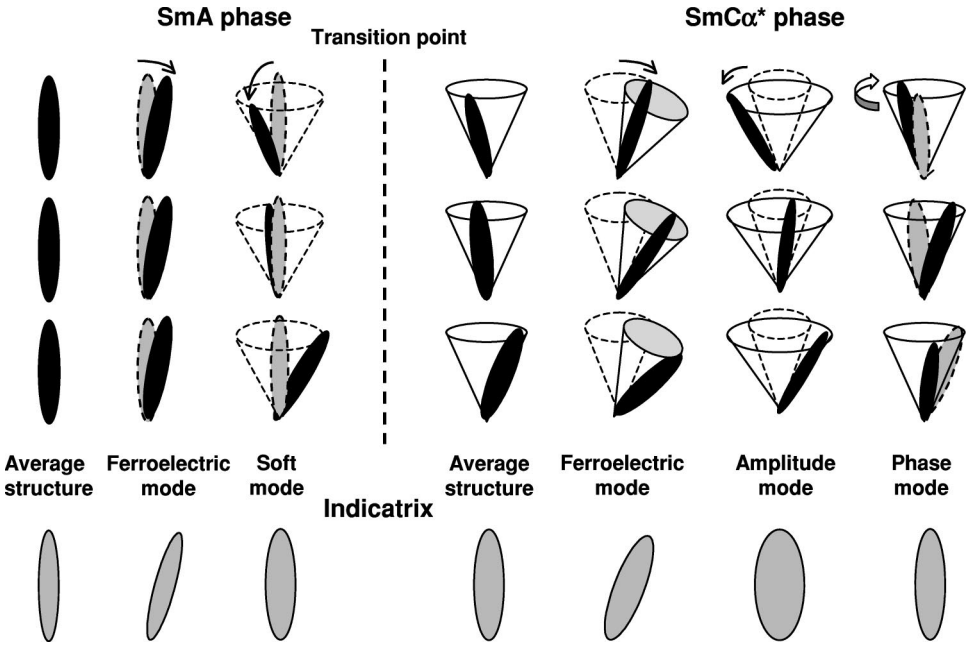


FIG. 1. Collective orientational modes related to the Sm-$A$–Sm-$C_\alpha^*$ phase transition. The change of the indicatrix induced by each mode is also described.

notice large soft mode fluctuations near the transition point in the Sm-$A$ phase. It was reported that especially in the Sm-$A$–Sm-$C_\alpha^*$ phase transition quite large pretransitional fluctuations were observed by means of heat capacity [8], birefringence [9], and layer compression modulus measurements [10]. We have also observed them by electro-optical [11] and third-order nonlinear dielectric measurements [12]. The responses increased remarkably in intensity as the transition point was approach in the Sm-$A$ phase. Theoretically, the second-order electro-optical and the third-order nonlinear dielectric responses are both proportional to the *susceptibility* of the amplitude mode [13]. In particular for the third-order nonlinear dielectric response, we have developed a theory under a dc field taking into account the pretransitional fluctuations to explain the experimental results [12]. The anomalous increase of intensity originates in the development of fluctuating large Sm-$C_\alpha^*$ phase domains near the transition point. These facts indicate that even in the Sm-$A$ phase we may observe the frequency dispersion in the third-order nonlinear dielectric response induced by the fluctuations in order to obtain the relaxation frequency of the soft mode. Quite recently, Orihara *et al.* [14] performed third-order nonlinear dielectric spectroscopy and succeeded in observing the soft mode condensation in the Sm-$A$ phase.

The amplitude mode in the Sm-$C_\alpha^*$ phase can also be observed by third-order dielectric spectroscopy. In this paper, we will present the complete results for the dynamic properties of the soft (amplitude) mode near the transition point in both the Sm-$A$ and Sm-$C_\alpha^*$ phases studied by means of linear and third-order nonlinear dielectric spectroscopy. In the next section, we develop a phenomenological theory and give the expressions for the linear and third-order nonlinear dielectric constants. The experimental procedures are described in the third section. In Sec. IV we present the experimental results and discuss them on the basis of the theory. Section V is devoted to conclusions.

## II. THEORY

In this section, we will present the Landau theory to analyze and explain the experimental results of third-order nonlinear dielectric spectroscopy in the Sm-$C_\alpha^*$ phase. As mentioned earlier, in the Sm-$A$ phase, we had to include fluctuations to develop a theory, but in the Sm-$C_\alpha^*$ phase the soft mode can be excited by an external electric field without fluctuations as will be seen later. On the other hand, in the Sm-$C_\alpha^*$ phase we need to include the sixth-order terms in the free energy to explain the temperature dependence of the third-order dielectric strength.

First, we define the order parameter in the $j$th smectic layer as $\vec{\xi}_j=(\xi_{jx},\xi_{jy})=(n_{jy}n_{jz},-n_{jx}n_{jz})$, where $\vec{n}_j=(n_{jx},n_{jy},n_{jz})$ is the director in the $j$th smectic layer and the $z$ axis is set to be along the layer normal. It is obvious that $\vec{\xi}_j$ is always parallel or antiparallel to the polarization. When we apply an electric field parallel to the smectic layer, we need to consider two kinds of liquid crystal molecular motion, a spatially homogeneous tilt, i.e., the ferroelectric mode $(\xi_{fx},\xi_{fy})$, and a helicoidal tilt, i.e., the soft mode $(\xi_1,\xi_2)$ related to the Sm-$A$–Sm-$C_\alpha^*$ phase transition, which is the primary order parameter in our case. With these modes we can express $\vec{\xi}_j$ as [7]

$$\xi_{jx}=\xi_{fx}+\xi_1\cos q_c jd-\xi_2\sin q_c jd, \tag{1a}$$

$$\xi_{jy}=\xi_{fy}+\xi_1\sin q_c jd+\xi_2\cos q_c jd, \tag{1b}$$

where $q_c$ is the wave number of the helicoidal structure and $d$ the layer spacing. The ferroelectric mode located at the Brillouin zone center is directly excited by the applied field through the piezoelectric coupling between the ferroelectric mode and the polarization, which contributes to the linear dielectric response. In the nonlinear third-order dielectric response, on the other hand, the nonlinear coupling between

the nonpolar soft mode and the ferroelectric mode plays an essential role, as well as the coupling between the soft mode and the applied field through the dielectric anisotropy. Taking these couplings into account, we can expand the free energy $f$ under an applied electric field as

$$f=\frac{a}{2}(\xi_1^2+\xi_2^2)+\frac{b}{4}(\xi_1^2+\xi_2^2)^2+\frac{c}{6}(\xi_1^2+\xi_2^2)^3+\frac{a_f'}{2}(\xi_{fx}^2+\xi_{fy}^2)+\frac{b_f}{4}(\xi_{fx}^2+\xi_{fy}^2)^2+\frac{\eta}{2}(\xi_1^2+\xi_2^2)(\xi_{fx}^2+\xi_{fy}^2)-\lambda_f(\xi_{fx}P_{fx}+\xi_{fy}P_{fy})+\frac{1}{2\chi_f}(P_{fx}^2+P_{fy}^2)-(P_{fx}E_x-P_{fy}E_y)-\frac{\varepsilon_a}{2}\left[\left\{\xi_{fy}^2+\frac{1}{2}(\xi_1^2+\xi_2^2)\right\}E_x^2-2\xi_{fx}\xi_{fy}E_xE_y+\left\{\xi_{fx}^2+\frac{1}{2}(\xi_1^2+\xi_2^2)\right\}E_y^2\right], \tag{2}$$

where $\varepsilon_a$ is the dielectric anisotropy at low frequencies and $\chi_f$ the dielectric susceptibility without the coupling between the polarization and ferroelectric order parameter. The $\eta$ term represents the nonlinear biquadratic coupling between the ferroelectric and soft modes. The coefficient $a$ is assumed to be linearly dependent on the temperature and becomes zero at the Sm-$A$–Sm-$C_\alpha^*$ transition point. $\lambda_f$ is the piezoelectric constant. Equilibrium conditions for the ferroelectric polarization $(P_{fx},P_{fy})$, $\partial f/\partial P_{fx}=\partial f/\partial P_{fy}=0$, yield

$$P_{fx}=\chi_f\lambda_f\xi_{fx}+\chi_fE_x, \tag{3a}$$

$$P_{fy}=\chi_f\lambda_f\xi_{fy}+\chi_fE_y. \tag{3b}$$

For convenience, we consider the case where the applied field is along the $x$ axis. Substituting Eq. (3a) into Eq. (2), we obtain

$$f=\frac{a}{2}(\xi_1^2+\xi_2^2)+\frac{b}{4}(\xi_1^2+\xi_2^2)^2+\frac{c}{6}(\xi_1^2+\xi_2^2)^3+\frac{a_f}{2}\xi_{fx}^2+\frac{b_f}{4}\xi_{fx}^4+\frac{\eta}{2}(\xi_1^2+\xi_2^2)\xi_{fx}^2-\chi_f\lambda_f\xi_{fx}E_x-\frac{\varepsilon_a}{4}(\xi_1^2+\xi_2^2)E_x^2, \tag{4}$$

where $a_f=a_f'-\chi_f\lambda_f^2$. We have dropped $\xi_{fy}$ because it cannot be excited by the field $E_x$. In the Sm-$C_\alpha^*$ phase, $\xi_1$ and $\xi_2$ may be changed by the applied field through nonlinear coupling and dielectric anisotropy. Without loss of generality we can put

$$\xi_1=\xi_s+\Delta\xi_1,\quad \xi_2=\Delta\xi_2, \tag{5}$$

where $\xi_s$ is the spontaneous value, and the field-induced parts $\Delta\xi_1$ and $\Delta\xi_2$ represent the amplitude mode and the phase mode (the Goldstone mode), respectively. From the equilibrium condition under no field in the Sm-$C_\alpha^*$ phase, $\partial f/\partial\xi_1=0$, $\xi_s$ is given as

$$a+b\xi_s^2+c\xi_s^4=0. \tag{6}$$

Substituting Eq. (5) into Eq. (4), we obtain the free energy for the amplitude mode up to second order in the Sm-$C_\alpha^*$ phase:

$$f=f_0+\frac{\tilde{a}}{2}\Delta\xi_1^2+\frac{\tilde{a}_f}{2}\xi_{fx}^2+\frac{b_f}{4}\xi_{fx}^4+\frac{\eta}{2}\xi_s\Delta\xi_1\xi_{fx}^2-\frac{\varepsilon_a}{4}\xi_s\Delta\xi_1E_x^2-\chi_f\lambda_f\xi_{fx}E_x, \tag{7}$$

where $\tilde{a}=a+3b\xi_s^2+5c\xi_s^4$ and $\tilde{a}_f=a_f+\eta\xi_s^2$, and $f_0$ is a constant independent of the amplitude and phase modes. We have omitted the higher-order terms, which contribute nothing to the third-order nonlinear dielectric response. Note that the above free energy does not include $\Delta\xi_2$, indicating that the relaxation frequency of the phase mode should be zero because it is the Goldstone mode, and it cannot be excited by an applied field. However, the relaxation frequency of the amplitude mode $\Delta\xi_1$ is finite and can be excited through linear-quadratic couplings between the soft and ferroelectric modes and between the soft mode and the applied electric field, which come from the biquadratic couplings in the Sm-$A$ phase. They play an important role in the third-order dielectric response as does the fourth-order term of the ferroelectric mode in the free energy, as shown below.

Next, we calculate the complex linear and nonlinear third-order dielectric constants under an ac field. From the above free energy we have the following Landau-Khalatnikov equation:

$$\gamma\frac{d\xi_{fx}}{dt}=-\frac{\partial f}{\partial\xi_{fx}}, \tag{8a}$$

$$\gamma\frac{d\Delta\xi_1}{dt}=-\frac{\partial f}{\partial\Delta\xi_1}, \tag{8b}$$

where we have assumed that the viscosity coefficient $\gamma$ for the soft mode should be the same as the one for the ferroelectric mode. Solving the above set of equations by the perturbation method with respect to $E_0$ under an ac field with frequency $\omega$ and amplitude $E_0$, i.e., $E_x=E_0\cos\omega t=E_0[\exp(i\omega t)+\text{c.c.}]/2$, we get up to third order

$$\Delta\xi_1=\chi_s(0)c_1(\omega)\xi_sE_0^2+\mathrm{Re}[\chi_s(2\omega)c_2(\omega)\exp(i2\omega t)]\xi_sE_0^2, \tag{9a}$$

$$\xi_{fx}=\mathrm{Re}[\chi_f\lambda_f\chi_f(\omega)E_0\exp(i\omega t)]-\mathrm{Re}[\{\eta\chi_f\lambda_f\xi_s^2\chi_s(2\omega)\chi_f(\omega)\chi_f(3\omega)c_2(\omega)+\tfrac{1}{4}b_f\chi_f^3\lambda_f^3\chi_f(3\omega)\chi_f^3(\omega)\}E_0^3\exp(i3\omega t)], \tag{9b}$$

with

$$c_1(\omega)=\frac{\varepsilon_a}{4}-\frac{1}{2}\eta\chi_f^2\lambda_f^2|\chi_f(\omega)|^2, \tag{10a}$$

$$c_2(\omega)=\frac{\varepsilon_a}{4}-\frac{1}{2}\eta\chi_f^2\lambda_f^2\chi_f^2(\omega), \tag{10b}$$

and

$$\chi_f(\omega)=(a_f+\eta\xi_s^2+i\omega\gamma)^{-1}, \tag{11a}$$

$$\chi_s(\omega)=(a+3b\xi_s^2+5c\xi^4+i\omega\gamma)^{-1}, \tag{11b}$$

where $\chi_f(\omega)$ and $\chi_s(\omega)$ are, respectively, the *linear* susceptibilities of the ferroelectric mode and the soft mode. From Eqs. (9a), (10a), and (10b) it is clearly seen that the amplitude mode can be excited through linear-quadratic couplings, is proportional to the square of the electric field in strength, and oscillates with the frequencies 0 and $2\omega$. Note that $\Delta\xi_1$ is proportional to $\xi_s$ and so the amplitude mode cannot be excited in the Sm-*A* phase without thermal fluctuations, as will be described later. The first term in Eq. (9b) contributes to the linear dielectric response. On the other hand, the second term contributes to the third-order dielectric response, which consists of two terms; the first one comes from the amplitude mode and the second one from the nonlinearity of the ferroelectric mode because it contains $b_f$. The polarization produced by the ferroelectric mode, $\xi_{fx}$, is obtained by substituting Eq. (9b) into the first term in Eq. (3a) as

$$\begin{aligned}P_{fx}=&\mathrm{Re}[(\chi_f^2\lambda_f^2\chi_f(\omega)+\chi_f)E_0\exp(i\omega t)]\\&-\mathrm{Re}[\{\eta\chi_f^2\lambda_f^2\xi_s^2\chi_s(2\omega)\chi_f(\omega)\chi_f(3\omega)c_2(\omega)\\&+\tfrac{1}{4}b_f\chi_f^4\lambda_f^4\chi_f(3\omega)\chi_f^3(\omega)\}E_0^3\exp(i3\omega t)].\end{aligned} \tag{12}$$

In addition to the above polarization due to the ferroelectric mode, we have to take into account the field-induced dipole of each molecule which comes from the dielectric anisotropy. The dielectric constant along the $x$ axis is expressed as

$$\varepsilon_{xx}=\varepsilon_\perp+\varepsilon_a\langle\xi_{jy}^2\rangle\simeq\varepsilon_\perp+\frac{\varepsilon_a}{2}\xi_s^2+\varepsilon_a\xi_s\Delta\xi_1 \tag{13}$$

where $\varepsilon_\perp$ is the dielectric constant perpendicular to the molecules. Therefore, we have the dielectric displacement due to the induced dipole of each molecule:

$$\begin{aligned}D^{(m)}=\varepsilon_{xx}E_x=\mathrm{Re}\Bigg[&\left(\varepsilon_\perp+\frac{\varepsilon_a}{2}\xi_s^2\right)E_0\exp(i\omega t)\\&+\frac{\varepsilon_a}{2}\xi_s^2\chi_s(2\omega)c_2(\omega)E_0^3\exp(i3\omega t)+\cdots\Bigg].\end{aligned} \tag{14}$$

Thus, we have the total dielectric displacement as

$$\begin{aligned}D_x=&D^{(m)}+P_{fx}\\=&\mathrm{Re}[\varepsilon_1(\omega)E_0\exp(i\omega t)+\varepsilon_3(\omega,\omega,\omega)E_0^3\\&\times\exp(i3\omega t)+\cdots]\end{aligned} \tag{15}$$

with

$$\varepsilon_1(\omega)=\chi_f+\varepsilon_\perp+\frac{\varepsilon_a}{2}\xi_s^2+\chi_f^2\lambda_f^2\chi_f(\omega), \tag{16a}$$

$$\begin{aligned}\varepsilon_3(\omega,\omega,\omega)=&2\xi_s^2\chi_s(2\omega)\left\{\frac{\varepsilon_a}{2}-\eta\chi_f^2\lambda_f^2\chi_f^2(\omega)\right\}\\&\times\left\{\frac{\varepsilon_a}{2}-\eta\chi_f^2\lambda_f^2\chi_f(\omega)\chi_f(3\omega)\right\}\\&-b_f\chi_f^4\lambda_f^4\chi_f(3\omega)\chi_f^3(\omega).\end{aligned} \tag{16b}$$

The last term in Eq. (16b) comes from the fourth-order term with respect to $\xi_{fx}$ in the free energy (7), i.e., the nonlinearity of the ferroelectric mode, which is well known in the nonlinear dielectric response [13]; it always exists irrespective of the fluctuations and the sign depends on $b_f$. On the other hand, the first term originates in the amplitude mode and is proportional to the *linear* susceptibility of the amplitude mode for $2\omega$, $\chi_s(2\omega)$.

## III. EXPERIMENT

The sample used in the present experiment was 4-(1-methyl-heptyloxycarbonyl)phenyl 4-octylcarbonyloxybiphenyl-4-carboxylate (MHPOCBC), the phase sequence of which is cryst–Sm-$I_A^*$–Sm-$C_A^*$–Sm-$C_\alpha^*$–Sm-*A*–iso [15]. In comparison with MHPOBC generally used in the study of the Sm-$C_\alpha^*$ phase, MHPOCBC has the merits that the Sm-$C_\alpha^*$ phase exists in quite a wide temperature interval, and the soft mode inducing the Sm-*A*–Sm-$C_\alpha^*$ phase transition and the ferroelectric soft mode are relatively different in relaxation frequency, as will be shown. The sample was introduced into a cell with indium tin oxide electrodes and polyimide layers in the isotropic phase and cooled down slowly to the Sm-*A* phase. The thickness was about 25 $\mu$m and the area of electrodes was $4\times4$ mm$^2$.

There is no measurement system commercially available for nonlinear dielectric spectroscopy. For our purpose, to study the dynamics in antiferroelectric liquid crystals, we have made a measurement system, the schematic of which is shown in Fig. 2. We used a charge amplifier and a vector signal analyzer with an oscillator (HP89410). A sinusoidal electric field was applied to the sample by the oscillator, and the output signal from the charge amplifier, which is proportional to the electric displacement in the sample, was analyzed with the vector signal analyzer to obtain the amplitudes and phases of the linear and third-order dielectric responses. The oscillator used in the measurements had higher-order harmonics and so their contributions were subtracted in the analyses. The cell was mounted in a hot stage (Instec HS1) and the temperature was controlled with an accuracy of 0.005 °C. The frequency dispersions were measured from 100 Hz to 1 MHz at stabilized temperatures in the cooling process. In the present experiment we performed nonlinear dielectric spectroscopy also in the Sm-*A* phase, where the third-order dielectric response exists only in a very narrow

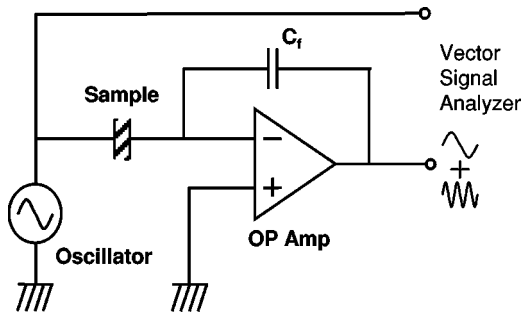


FIG. 2. Schematic diagram of the linear and nonlinear dielectric measurement system used in the present experiment.

temperature range near the transition point. Therefore, we performed the measurements with a step of 0.02 °C.

In general, when a cosine electric field $E=E_0\cos\omega t$ is applied to the sample, the electric displacement $D$ can be expressed in terms of linear and nonlinear dielectric constants as

$$D=\left\{\varepsilon_1(\omega)\left(\frac{E_0}{2}\right)+3\varepsilon_3(\omega,\omega,-\omega)\left(\frac{E_0}{2}\right)^3+\cdots\right\}\exp(i\omega t)$$
$$+\left\{\varepsilon_3(\omega,\omega,\omega)\left(\frac{E_0}{2}\right)^3+5\varepsilon_5(\omega,\omega,\omega,\omega,-\omega)\left(\frac{E_0}{2}\right)^5\right.$$
$$\left.+\cdots\right\}\exp(i3\omega t)+\cdots+\text{c.c.}, \qquad (17)$$

where we have assumed that the sample is nonpolar, i.e., for reasons of symmetry the even-order terms with respect to the field strength disappear. In the above expression, $\varepsilon_1(\omega)$ is the linear dielectric constant and the other coefficients are nonlinear dielectric constants. In the present experiments we measured the linear dielectric constant $\varepsilon_1(\omega)$ and the third-order dielectric constant $\varepsilon_3(\omega,\omega,\omega)$. From this equation it is clear that in the actual measurements it is necessary to check the linearity between the $n$th-order response $D_n$ and $E_0^n$ when we would like to obtain $\varepsilon_n(\omega,\ldots,\omega)$. Otherwise, the higher-order contributions are included and the correct value cannot be obtained.

## IV. RESULTS AND DISCUSSION

First, we show in Fig. 3 the dependences of the complex electric displacements $D_n$ on $E_0^n$ at 102.1 °C just below the Sm-$A$–Sm-$C_\alpha^*$ phase transition point to check the linearity of the dielectric response. Here $D_1$ and $D_3$ are the first- and the third-order harmonics of $D$, i.e., the coefficients of $\exp(i\omega t)$ and $\exp(3i\omega t)$, respectively. In the measured electric field range, it was confirmed that both the real and imaginary parts of the electric displacements $D_n$ have linear relations with the electric field $E_0^n$, indicating that there is no contribution from the higher-order terms and we can correctly measure $\varepsilon_1(\omega)$ and $\varepsilon_3(\omega,\omega,\omega)$ from the slope. When we measured the temperature dependence of dielectric dispersions we applied only one value of field strength, which was determined

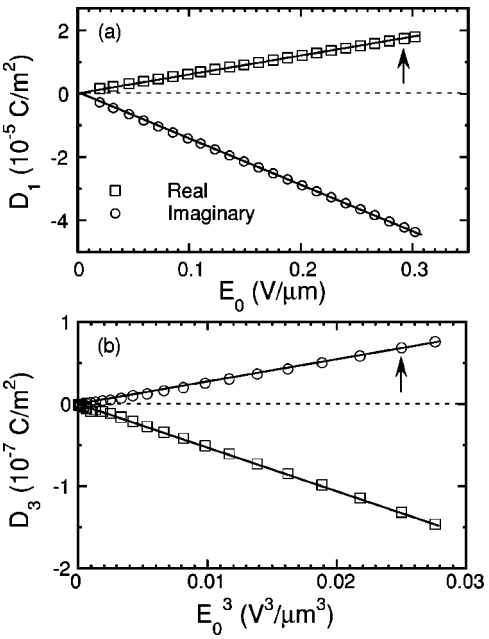


FIG. 3. Dependences of the real and imaginary parts of (a) $D_1$ and (b) $D_3$ on $E_0^n$, measured simultaneously at 1 kHz at 102.10 °C just below the Sm-$A$–Sm-$C_\alpha^*$ phase transition point. The solid lines are the best fitting results of $D_n=\varepsilon_n E_0^n$.

to be 0.292 V/$\mu$m from Fig. 3 and is indicated by arrows therein.

Figure 4 shows the temperature dependences of the real parts of the linear and third-order dielectric constants measured at 1 kHz. Both the linear and third-order dielectric constants have peaks around the transition point, but their peak positions do not coincide. Therefore, we determined the Sm-$A$–Sm-$C_\alpha^*$ phase transition point from the inflection point in the temperature dependence of the birefringence. Precise measurements of the birefringence have been made by Skarabot *et al.* and they observed a sudden change of the slope at the transition point [2]. As a result of the simultaneous dielectric and birefringence measurements, it has been clarified that the peak temperature of the linear dielectric constant corresponds to the transition temperature (102.26 °C) as shown in Fig. 4. The details of the simulta-

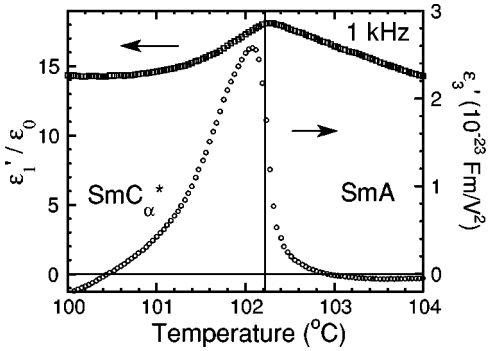


FIG. 4. Temperature dependences of the real parts of $\varepsilon_1(\omega)$ and $\varepsilon_3(\omega,\omega,\omega)$ measured simultaneously at 1 kHz in the cooling process.

neous measurements will be reported elsewhere [16].

The linear dielectric constant increases gradually in the Sm-*A* phase as the transition point is approached, and takes a maximum, and then it decreases in the Sm-$C_\alpha^*$ phase, as has been reported by Isozaki *et al.* [15]. From Eqs. (16a) and (11a), which are also valid in the Sm-*A* phase when we put $\xi_s=0$ [14], it is easily seen that the linear dielectric constant has a linear relationship to the susceptibility of the ferroelectric mode, $\chi_f(\omega)$. Therefore, this gradual increase with decreasing temperature in the Sm-*A* phase indicates the partial softening of the ferroelectric mode. This will be made clearer by the temperature dependence of its relaxation frequency as shown later. In the third-order dielectric response, on the other hand, the temperature dependence is more complicated. At high temperatures far from the transition point in the Sm-*A* phase the real part is negative and increases with decreasing temperature, and then it becomes zero above the transition point and changes sign to positive. In the vicinity of the transition point it increases steeply and has a peak below the transition temperature in the Sm-$C_\alpha^*$ phase, and then it decreases with decreasing temperature. The steep increase of the third-order dielectric response near the transition point in the Sm-*A* phase has been explained by a theory that takes into account the pretransitional fluctuations [12]. However, it can be roughly explained by Eq. (16b), if we replace $\xi_s^2$ by its thermal average. In Eq. (16b) there are two contributions to the third-order dielectric constant; one comes from the soft mode and the other from the fourth-order term with respect to $\xi_{fx}$ in Eq. (7). The former is positive and proportional to the mean square fluctuation for this case and so it takes positive large values near the transition point because of the pretransitional fluctuations, while the sign of the latter depends on the coefficient $b_f$, which is considered to be positive since $\varepsilon_3$ is negative far from the transition point where the fluctuations are negligibly small. These facts can also explain the sign inversion of the third-order dielectric constant in the Sm-*A* phase.

We show the temperature dependence of the frequency dispersion of $\varepsilon_3''(\omega)$, which is defined as $-\mathrm{Im}(\varepsilon_3)$, in the vicinity of the Sm-*A*–Sm-$C_\alpha^*$ phase transition point in Fig. 5, where the temperature step is 0.02 °C. We can clearly see the softening of the soft mode in both the Sm-*A* and Sm-$C_\alpha^*$ phases and the peak frequency has a minimum at about 102.26 °C (the corresponding dispersion curve is shown by a bold line), which corresponds to the peak temperature of the linear dielectric constant. The actual relaxation frequency should be obtained by a least-squares fit using the formula derived theoretically.

Figure 6 shows the typical frequency dispersions of the linear dielectric constant $\varepsilon_1$ and the third-order dielectric constant $\varepsilon_3$ in the Sm-*A* phase (102.30 °C). It is seen from Fig. 6(a) that only the ferroelectric mode is involved in the linear dielectric constant in the measured frequency region. The increase of dielectric constant at low frequency should be due to ionic conduction. In our analysis, therefore, we modified Eq. (16a) to

$$\varepsilon_1(\omega)=\varepsilon_\infty+\frac{\Delta\chi_f}{1+(i\omega\tau_f)^{\beta_f}}+\frac{1}{(i\omega\tau_i)^{\delta}}, \qquad (18)$$

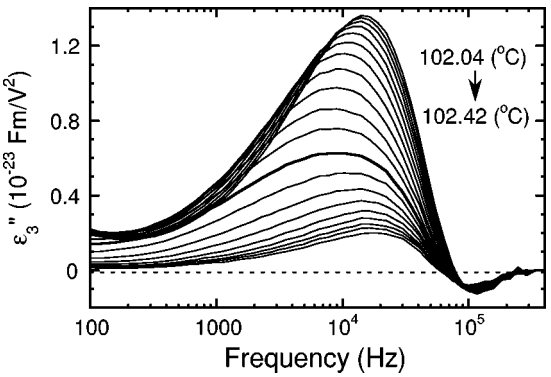


FIG. 5. Temperature dependence of the frequency dispersion in $\varepsilon_3''(\omega)$. The transition point is about 102.26 °C and the corresponding frequency dispersion is drawn by a bold line.

where the last term has been added to take the conductivity into account, and $\tau_f=\gamma/(a_f+\eta\xi_s^2)$ is the relaxation time of the ferroelectric mode, $\varepsilon_\infty$ is the dielectric constant at the high-frequency limit, $\Delta\chi_f$ is the dielectric strength, and $\beta_f$ and $\delta$ are distribution parameters. The fit result using the least-squares method is shown by solid lines in Fig. 6(a). A good agreement was obtained. The distribution parameter $\beta_f$ was almost 1. In the third-order dielectric response shown in Fig. 6(b), on the other hand, the frequency dispersion is quite different from that of the linear one. Orihara *et al.* [14] have made a detailed analysis of the frequency dispersion of the third-order dielectric response in the Sm-*A* phase on the basis of a formula derived from the Langevin equation taking into account the pretransitional fluctuations. According to their results, $\varepsilon_3$ in the Sm-*A* phase is obtained by replacing $\xi_s^2\chi_s(2\omega)$ in Eq. (16b) by

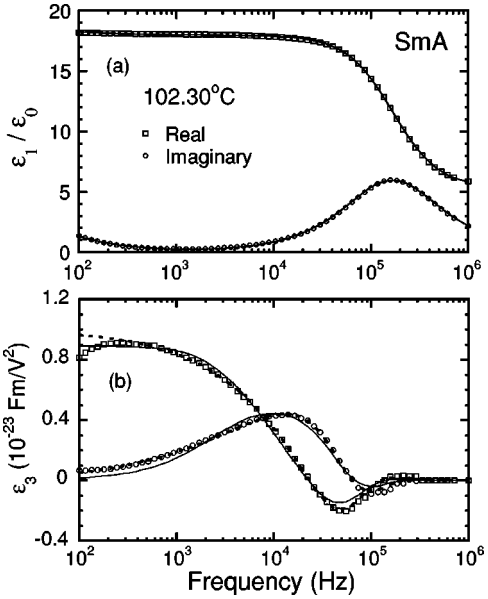


FIG. 6. Typical frequency dispersions of (a) $\varepsilon_1(\omega)$ and (b) $\varepsilon_3(\omega,\omega,\omega)$ obtained in the Sm-*A* phase (102.30 °C). The solid lines represent the best fit results with Eq. (18) and Eq. (21) for the linear and the third-order nonlinear dielectric dispersions, respectively. In (b), the broken line is the best fit with the distribution parameter $\beta$.

$$C|T-T_c|^{-1/2}g(i\omega\tau_s), \tag{19}$$

with

$$g(Z)=\frac{2(\sqrt{1+Z}-1)}{Z}, \tag{20}$$

where $C$ is a constant and $\tau_s$ is the relaxation frequency of the soft mode. When the above equation was derived it was assumed that not only the soft mode located at $q_c$ in the smectic Brillouin zone but also the modes around $q_c$ contribute to the third-order dielectric response and the soft mode branch has a parabolic dispersion around $q_c$. Therefore, $g(i\omega\tau_s)$ has a wide distribution of relaxation times. We used the following formula for the fitting of $\varepsilon_3$ in the Sm-$A$ phase:

$$\varepsilon_3(\omega,\omega,\omega)=g(i\omega\tau_s)\left(A_{s1}-\frac{A_{s2}}{(1+i\omega\tau_f)^2}\right)\times\left(A_{s1}-\frac{A_{s2}}{(1+i\omega\tau_f)(1+i3\omega\tau_f)}\right)+\frac{A_f}{(1+i3\omega\tau_f)(1+i\omega\tau_f)^3}. \tag{21}$$

Since the contribution from the dielectric anisotropy term $A_{s1}$ in our present experiment was small, we fixed it to be zero to obtain better stability in the fitting process. The solid lines in Fig. 6(b) represent the best fit with the above formula, where we fixed $\tau_f$ to be the same value determined from $\varepsilon_1$. At low frequencies the agreement between the theory and the experiment is not good. This is improved by introducing $\beta$ in Eq. (21); by replacing $i\omega\tau_s$ by $(i\omega\tau_s)^{\beta_s}$. The parameter $\beta_s$ causes a distribution of relaxation frequency as in the Cole-Cole function $1/[1+(i\omega\tau_s)^{\beta}]$. The fit result is shown by the broken lines in Fig. 6(b). The agreement becomes much better. This result indicates that we need another distribution, although the function $g(i\omega\tau_s)$ itself has a distribution as described above. The discrepancy may originate from the temperature distribution in the sample. However, we have to mention another possibility, that in principle $g(i\omega\tau_s)$ should have a broader distribution since we have used a few assumptions such as the Gaussian approximation and the parabolic dispersion in deriving Eq. (21). The origin is not yet clear. In addition, it was seen that $\tau_s$ strongly depends on $\beta_s$. Therefore, we used $g(i\omega\tau_s)$ without $\beta_s$ when we analyzed the data to obtain the relaxation frequency of the soft mode. Here, it should be noted that even if we introduce $\beta_s$ the deviation from the data remains at very low frequencies. This may be due to the ionic conductivity or another mode in the low-frequency region, which has been observed also by electro-optical measurement in the Sm-$C^*_\alpha$ phase [7].

Next, we show the typical frequency dispersions in the Sm-$C^*_\alpha$ phase in Fig. 7. In the linear dielectric response (a), only the ferroelectric mode is observed as in the Sm-$A$ phase and is well fitted by using Eq. (18). The dispersion curve of the third-order dielectric response is shown in Fig. 7(b).

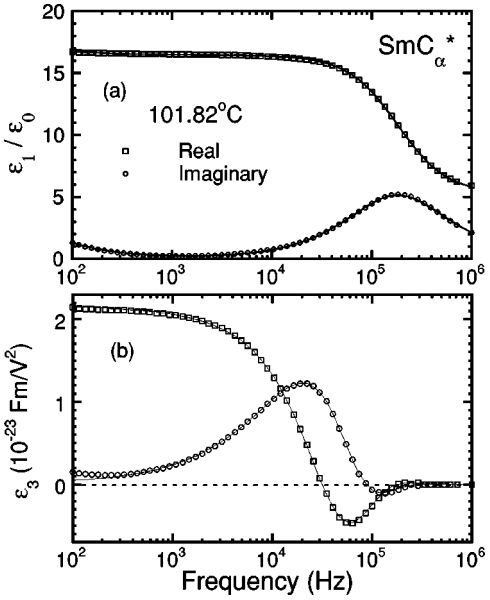


FIG. 7. Typical frequency dispersions of (a) $\varepsilon_1(\omega)$ and (b) $\varepsilon_3(\omega,\omega,\omega)$ obtained at 101.82 °C in the Sm-$C^*_\alpha$ phase. The solid lines represent the best fit results with Eq. (18) and Eq. (22) for the linear and third-order nonlinear dielectric dispersions, respectively.

From Eqs. (16b), (11a), (11b), (10a), and (10b), it is easily seen that the expression for $\varepsilon_3$ in the SmC$^*_\alpha$ for the fitting is given by

$$\varepsilon_3(\omega,\omega,\omega)=\frac{1}{1+(i2\omega\tau_s)^{\beta_s}}\left(A_{s1}-\frac{A_{s2}}{(1+i\omega\tau_f)^2}\right)\times\left(A_{s1}-\frac{A_{s2}}{(1+i\omega\tau_f)(1+i3\omega\tau_f)}\right)+\frac{A_f}{(1+i3\omega\tau_f)(1+i\omega\tau_f)^3}, \tag{22}$$

where $\tau_s=\gamma/(a+3b\xi_s^2+5c\xi_s^4)$ is the relaxation time of the soft mode (the amplitude mode) and a distribution parameter $\beta_s$ has been introduced. Note that Eq. (22) is obtained from Eq. (21) by replacing $g(i\omega\tau_s)$ by $1/[1+(i2\omega\tau_s)^{\beta_s}]$. The fitting procedure in the Sm-$C^*_\alpha$ phase was the same as that in the Sm-$A$ phase. The solid line in Fig. 7(b) is a theoretical curve and a good agreement is obtained between the experiment and the theory.

Figure 8 shows the temperature dependences of the relaxation frequencies of the ferroelectric mode and the soft mode, $f_{r,f}=(2\pi\tau_f)^{-1}$ and $f_{r,s}=(2\pi\tau_s)^{-1}$, obtained from the fitting. In the Sm-$A$ phase the relaxation frequency of the soft mode, $f_{r,s}$, decreases as the transition point is approached and becomes almost zero at the transition point, namely, soft mode condensation takes place, and in the Sm-$C^*_\alpha$ phase the relaxation frequency of the soft mode (the amplitude mode) increases with decreasing temperature. The Curie-Weiss law holds for these modes. Thus, the soft mode (the amplitude mode) has been observed in the vicinity of the Sm-$A$–Sm-$C^*_\alpha$ phase transition point. For the ferroelectric

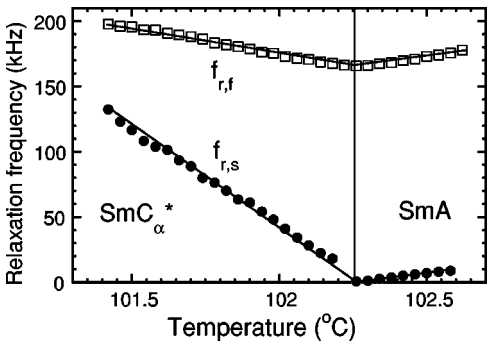


FIG. 8. Temperature dependences of the relaxation frequencies obtained from the linear and the third-order nonlinear dielectric spectroscopy. $f_{r,f}$ and $f_{r,s}$ are the relaxation frequencies of the ferroelectric mode and the soft mode, respectively.

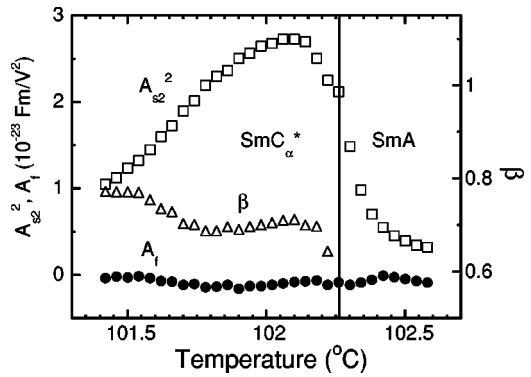


FIG. 9. Temperature dependences of adjustable parameters.

mode, on the other hand, partial softening is seen in the Sm-*A* phase. This fact and the relation $\tau_f=\gamma/(a_f+\eta\xi_s^2)$ with $\xi_s=0$ indicate that $a_f$ should decrease as the temperature is decreased. In the Sm-$C_\alpha^*$ phase the relaxation frequency increases, indicating that $\eta$ should be positive. Here, it should be noted that the slope of the soft mode (146 kHz/°C) in the Sm-$C_\alpha^*$ phase is about four times larger than that in the Sm-*A* phase (34 kHz/°C). This result indicates that the Sm-*A*–Sm-$C_\alpha^*$ phase transition should be close to the tricritical point, where the fourth-order coefficient in the Landau expansion vanishes and the slope ratio becomes 4 [17], as has been pointed out by Skarabot *et al.* [2]. In addition, the slopes of the soft and ferroelectric modes in the Sm-*A* phase are almost the same; the latter is 38 kHz/°C. This result was assumed in our previous paper when we discussed the validity of a discrete model proposed by Sun *et al.* [18] to explain the dynamics of phase transitions in antiferroelectric liquid crystals. In the model the transitions to tilted phases from the Sm-*A* phase are assumed to take place in each layer even without interactions between neighboring layers, leading to the result that the doubly degenerate dispersion branch in the Sm-*A* phase goes down without changing shape as the temperature is decreased in the Sm-*A* phase, i.e., the slope of the relaxation frequency vs the temperature measured at any point in the smectic Brillouin zone should be the same. In the present case this means that $a_f=a+b$, where $b$ is a temperature-independent positive constant.

The other parameters obtained from the least-squares fitting are shown in Fig. 9. It is seen that $A_f$ $(\propto -b_f)$ takes a small negative value independent of the temperature, indicating that the contribution of the fourth-order term of the ferroelectric mode is quite small. In Fig. 9, $A_{s2}^2$ was plotted instead of $A_{s2}$ itself since it is the third-order dielectric strength and is proportional to the soft mode strength $\chi_s(0)$. Compared with $A_f$, $A_{s2}^2$ is positive as it should be and becomes large near the transition point. The temperature dependence of $A_{s2}^2$ is quite similar to that of $\varepsilon_3'$ at 1 kHz shown in Fig. 3. In the Sm-$C_\alpha^*$ phase $A_{s2}^2$ takes a peak value inside, not at the transition point. This behavior cannot be explained by the present theory. From Eqs. (16b), (6), and (11b) it is seen that near the transition point in the Sm-$C_\alpha^*$ phase $A_{s2}^2\propto\xi_s^2\chi_s(0)$ $\propto(b+2c\xi_s^2)^{-1}$, where we have put $A_{s1}(\varepsilon_a)=0$. Since the Sm-*A*–Sm-$C_\alpha^*$ phase transition is of second order, $b$ is positive. When $c$ is positive, $A_{s2}^2$ should decrease monotonically with decreasing temperature. In this case, it is not possible to explain the increase just below the transition point, but it might be possible by taking into account the nonlinearity and the large fluctuations. Just below the transition point many phase defects, which appear due to the phase mismatch of the order parameter, may be excited. These defects can make an additional contribution to the third-order dielectric constant. On the contrary, when $c$ is negative $A_{s2}^2$ should increase monotonically. If we regard this increase as the one experimentally observed just below the transition point, the following decrease may be reproduced by introducing higher-order terms in the free energy within the Landau theory without fluctuations, although this is not a plausible explanation. In order to clarify the origin of the anomaly just below the transition point it may be necessary to study the effect of fluctuations in the third-order response in the Sm-$C_\alpha^*$ phase. The anomaly can also be seen, in the temperature dependence of $\beta_s$; as the transition point is approached $\beta_s$ decreases remarkably just below it.

## V. CONCLUSIONS

We have performed linear and the third-order nonlinear dielectric spectroscopies in an antiferroelectric liquid crystal 4-(1-methyl-heptyloxycarbonyl)phenyl 4-octylcarbonyloxybiphenil-4-carboxylate. A Landau-type theory was developed to analyze the frequency dispersions. By utilizing the theory we have succeeded in obtaining the relaxation frequency of the soft mode (the amplitude mode) in both the Sm-*A* and Sm-$C_\alpha^*$ phases. The relaxation frequency obeys the Curie-Weiss law in both phases and therefore this is direct evidence that the Sm-*A*–Sm$C_\alpha^*$ phase transition is brought about by the soft mode condensation of an overdamped collective mode. Furthermore, from the slopes of the relaxation frequencies of the soft mode (the amplitude mode) and the ferroelectric mode, we conclude directly that the Sm-*A*–Sm$C_\alpha^*$ phase transition is close to a tricritical point, and the discrete model, in which the transitions to tilted phases from the Sm-*A* phase take place in each layer even without interactions between neighboring layers, is

valid. At the end of this paper we would like to emphasize that nonlinear dielectric spectroscopy has the outstanding merit that we can use it to measure the frequency dispersion of nonpolar soft modes, not only in the tilted phases but also in the Sm-*A* phase if the pretransitional fluctuations are large.

**ACKNOWLEDGMENTS**

We would like to thank Showa Shell Sekiyu Co. Ltd. for supplying MHPOCBC. This study was partly supported by Grants-in-Aid from the Ministry of Education, Science, Sports and Culture (Grant Nos. 11099724 and 12650882).

[1] T. Isozaki, K. Hiraoka, Y. Takanishi, H. Takezoe, A. Fukuda, Y. Suzuki, and I. Kawamura, Liq. Cryst. **12**, 59 (1992).
[2] M. Škarabot, M. Čepič, B. Žekš, R. Blinc, G. Heppke, A.V. Kityk, and I. Muševič, Phys. Rev. E **58**, 575 (1998).
[3] P. Mach, R. Pindak, A.-M. Levelut, P. Barois, H.T. Nguyen, C.C. Huang, and L. Furenlid, Phys. Rev. Lett. **81**, 1015 (1998).
[4] P. Mach, R. Pindak, A.-M. Levelut, P. Barois, H.T. Nguyen, H. Baltes, M. Hird, K. Toyne, A. Seed, J.W. Goodby, C.C. Huang, and L. Furenlid, Phys. Rev. E **60**, 6793 (1999).
[5] S.M. Khened, S. Krishna Prasad, B. Shivkumar, and B.K. Sadashiva, J. Phys. II **1**, 171 (1991).
[6] I. Muševič, R. Blinc, B. Žekš, C. Filipič, M. Čopič, A. Seppen, P. Wyder, and A. Levanyuk, Phys. Rev. Lett. **60**, 1530 (1988).
[7] V. Bourny, A. Fajar, and H. Orihara, Phys. Rev. E **62**, R5903 (2000).
[8] K. Ema and H. Yao, Phys. Rev. E **57**, 6677 (1998).
[9] M. Škarabot, K. Kočevar, R. Blinc, G. Heppke, and I. Muševič, Phys. Rev. E **59**, R1323 (1999).
[10] S. Shibahara, J. Yamamoto, Y. Takanishi, K. Ishikawa, H. Takezoe, and H. Tanaka, Phys. Rev. Lett. **85**, 1670 (2000).
[11] A. Fajar, H. Orihara, V. Bourny, J. Pavel, and V. Lorman, Jpn. J. Appl. Phys., Part 2 **39**, L166 (2000).
[12] H. Murai, V. Bourny, A. Fajar, and H. Orihara, Mol. Cryst. Liq. Cryst. Sci. Technol. Sect. A **364**, 645 (2001).
[13] H. Orihara and Y. Ishibashi, J. Phys. Soc. Jpn. **64**, 3775 (1995).
[14] H. Orihara, A. Fajar, and V. Bourny, Phys. Rev. E **65**, 040701 (2002).
[15] T. Isozaki, Y. Suzuki, I. Kawamura, K. Mori, N. Nakamura, N. Yamamoto, Y. Yamada, H. Orihara, and Y. Ishibashi, Jpn. J. Appl. Phys., Part 2 **30**, L1573 (1991).
[16] A. Fajar and H. Orihara (unpublished).
[17] R. Blinc and B. Žekš, *Soft Modes in Ferroelectrics and Antiferroelectrics* (North-Holland, Amsterdam, 1974).
[18] H. Sun, H. Orihara, and Y. Ishibashi, J. Phys. Soc. Jpn. **62**, 2706 (1993).